Proceedings of the 9th U.S. National and 10th Canadian Conference on Earthquake Engineering
Compte Rendu de la 9ième Conférence Nationale Américaine et
10ième Conférence Canadienne de Génie Parasismique
July 25-29, 2010, Toronto, Ontario, Canada • Paper No 1767

INFLUENCE OF SPECTRAL NONSTATIONARITY ON STRUCTURAL DAMAGE

S.D. Koduru[1]

ABSTRACT

Spectral nonstationarity is the time dependent evolution in the frequency content of an earthquake ground motion. The traditional earthquake demand measures such as the response spectra and the Fourier amplitude spectra do not consider this time dependent variability in the frequency content. Hence, the ground motions based solely on these measures may underestimate the nonlinear response of a structure. This study demonstrates that the relative lag in the arrival time of the low frequency waves would increase the structure damage. The structural damage is measured in terms of cumulative damage indices, which include the effect of duration and the number of load cycles. The numerical example with a six storey reinforced concrete frame illustrates the increment of damage due to the effect of spectral nonstationarity.

Introduction

The earthquake ground motions form a critical component of the performance-based earthquake engineering (PBEE) due to its emphasis on the evaluation of inelastic behaviour of the structures. In most cases, the earthquake ground motion records satisfying the criteria of earthquake magnitude, distance, source characteristics, geology, and site-soil conditions are scarce. Consequently, in order to select ground motions, the following two approaches are commonly employed; 1) ground motion records are scaled such that their response spectra match a "design spectrum" or a "uniform hazard spectrum," 2) artificial ground motions are simulated based on stochastic models.

In the first approach, the emphasis is to match the amplitude of frequency content in a ground motion record to the design level. This approach is valuable for predicting the peak elastic response of the structure. However, it does not consider the time dependent factors within the earthquake ground motions such as, duration and the evolution of the frequency content, which may significantly affect the inelastic response of the structure.

For the second approach, the stochastic models may broadly be categorized as "source-based" and "site-based" (Rezaeian and Der Kiureghian 2008). In the source-based stochastic models, the focus is yet again on the amplitude of the frequency content of the ground motions. These models include only the variation of earthquake intensity with time, known as "temporal

---

[1] Engineer 1, Civil Design – Structural Team, BC Hydro, Burnaby, V3N 4X8 BC Canada

nonstationarity." The time dependent variation of the frequencies, known as "spectral nonstationarity," is not explicitly modeled. Thus, most of these models result in stationary frequency content in the ground motions. The site-based stochastic models, on the other hand, focus on representing the temporal and spectral nonstationarity observed in the ground motion records.

The spectral nonstationarity occurs partly due to the irregular rupturing of the earthquake faults and partly due to arrival of the high frequency seismic waves at a location earlier than the low frequency waves. In the nonlinear response range, the natural frequency of the structure decreases as it loses stiffness. The low frequency content at the end of ground motion would then potentially increases the damage of the structure due to the moving resonance effect (Conte 1992).

In the present study, the effect of the spectral nonstationarity on the structural damage is investigated with cumulative damage indices. This differs from the previous studies that focus on the influence of spectral nonstationarity on inelastic displacement response (Conte 1992), strength reduction factors (Mukherjee and Gupta 2002), peak response parameters (Wang et al. 2002, Cao and Friswell 2009), and collapse time (Todorovska et al 2009). Moreover, the parameters of the hysteretic material models that amplify the spectral nonstationarity effects are identified.

In the following, the quantitative measures for spectral nonstationarity and the parameters to simulate ground motions with spectral nonstationarity are discussed. Next, the hysteretic material models, cumulative damage measures and the "damage spectra" for the ground motions with stationary and nonstationary frequency content are presented. Finally, the influence of spectral nonstationarity on the structural damage of a six storey building is studied.

Spectral Nonstationarity Measures

For the time-frequency decomposition of a ground motion, signal processing methods such as short-time Fourier transform, chirplet-based signal approximation, and wavelets are well-known. In particular, the wavelet methods have gained popularity for their representation of energy variation in time-frequency plane. In recent years, the wavelet methods are explored for ground motion simulation models and nonstationarity representation (Iyama and Kuwamura 1999, Mukherjee and Gupta 2002, Cao and Friswell 2009, Todorovska et al. 2009). Alternatively, unwrapping phase spectra of the well-known Fourier transform provides another measure of spectral nonstationarity. It represents the lag in the arrival times of various frequencies at the recording site. The phase differences are widely used to characterize the relative arrival times of various frequencies (Shrikand and Gupta 2001, Thrainsson and Kiremidjian 2002).

In the present study, the "envelope delay" proposed by Boore (2003) is utilized as a measure of spectral nonstationarity. The envelope delay is the derivative of phase with respect to frequency and is interpreted as the arrival time of seismic waves. Thus, envelope delay presents an intuitive measure of nonstationarity. Moreover, it is computed employing only the Fourier transforms and without unwrapping the phase.

If $h(t)$ represents a ground motion record, $H(f)$, its Fourier transform and $G(f)$ is the Fourier transform of $t.h(t)$ with t as time and f as frequency, then the envelope delay, $t_e(f)$ is (Boore 2003)

$$t_e(f) = \frac{1}{2\pi}\frac{d\phi}{df} = \frac{R(H)\cdot R(G)+I(H)\cdot I(G)}{A^2} \tag{1}$$

where ϕ is the phase, $R(H)$ and $I(H)$ are the real and imaginary parts of $H(f)$, $R(G)$ and $I(G)$ are the real and imaginary parts of $G(f)$, and A is the Fourier amplitude of f. Fig. 1 shows the envelope delays plotted with frequencies in log scale for the ground motion records of Northridge earthquake (090 component,116th St School station), and Loma Prieta earthquake (00 component, APEEL 7-Pulgas station) (the ground motion records are obtained from http://peer.berkeley.edu/nga/). Evidently, the Northridge record displays longer envelope delays for low frequency content compared to the Loma Prieta record.
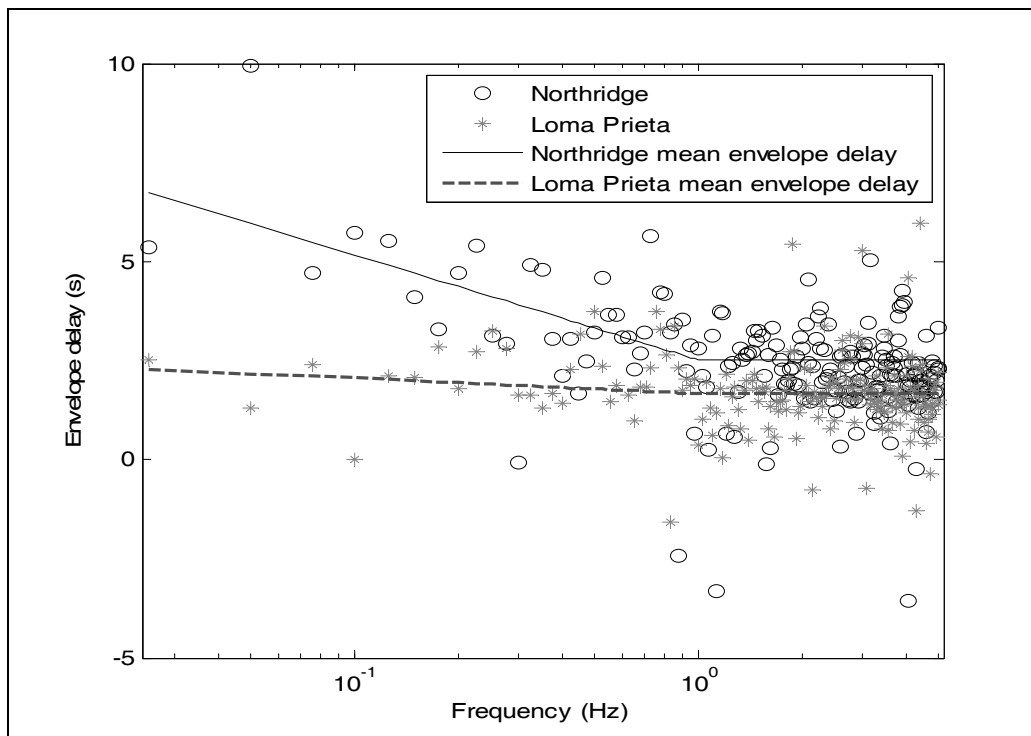

Figure 1. Envelope delays for the Northridge earthquake record and the Loma Prieta earthquake record

A bilinear curve, called "mean envelope delay," is fitted to the envelope delays in Fig. 1 to compare the nonstationarity of the two records. For frequencies less than 1Hz, the slope of the mean envelope delay for the Northridge record is -2.65, while the slope for the Loma Prieta record is -0.172. Therefore, the higher slope indicates longer delays in the arrival of the low frequency content. Thus, the slope for the frequency content less than 1Hz provides a quantitative measure of comparison for the spectral nonstationarity.

Ground Motion Model

A review of the stochastic models with temporal and spectral nonstationarity is presented in Koduru (2008). In the present study, the stochastic model proposed by Li and Der Kiureghian (1995) is employed. It represents the ground motion as a summation of several filtered Gaussian white noise processes. The discretized form of the simulated ground motion, $x(t)$, is then

$$x(t) = \sum_{k=1}^{M} q_k(t)s_k(t) \tag{2}$$

where $q_k(t)$ is a modulating function that controls the variation of intensity of a stationary process $s_k(t)$ over time, t. The stationary process is simulated as,

$$s_k(t) = \sum_{i=1}^{N} y_{ki}h_k(t-t_i) \tag{3}$$

where y_{ki} is a standard normal random variable, which represents a pulse in the Gaussian white noise process, and $h_k(t-t_i)$ represents an impulse response function, which acts as a filter with frequency, ω_k and damping ratio, ξ_k. Thus, $s_k(t)$ represents a stationary process with a dominant frequency ω_k and band width controlled by ξ_k. Modulating functions are able to take a number of functional forms to control the temporal evolution of stationary processes. Each modulating function is associated with a stationary process and hence with a unique filter.

The calibration of ω_k, ξ_k. and $q_k(t)$, to a ground motion record would enable to simulate an ensemble of ground motions with Eq. (2). Following the calibration procedure outlined in Koduru (2008), the parameters of the stochastic model are assessed for the Loma Prieta earthquake record. Five filters are chosen with dominant frequencies, 0.33Hz, 1.59Hz, 2.50Hz, 5.19Hz and 53.13Hz, and with damping ratios as 0.1 for the first two filters and 0.2 for the rest of them. Initially, the modulating functions corresponding to each filter are calibrated as piece-wise linear functions. For the first two filters, which represent the low frequency content, the modulating functions are then modified to represent triangular function. The triangular modulating function is fully defined by only four parameters, which are, arrival time, peak amplitude, the location of peak amplitude and the duration. Thus, the sensitivity of structural response to each of the parameter could be easily illustrated. In this paper, the study is confined to the influence of the arrival times on the structural damage. Fig. 2 shows the five modulating functions corresponding to each filter.

Employing the parameters in Fig. 2, a set of 100 ground motions is simulated with the stochastic model in Eq. (2). This is termed as "Model 1" in the paper for easy reference. Another set of 100 ground motions is simulated with 5s delayed arrival time for the modulating function of 0.33Hz filter. This is termed as "Model 2" in the paper. All the simulations are passed through a high pass filter corresponding to the high pass filter of the target ground motion record. The simulated ground motions based on Model 2 should exhibit higher spectral nonstationarity than the ground motions based on Model 1 due to the delay in the arrival time.
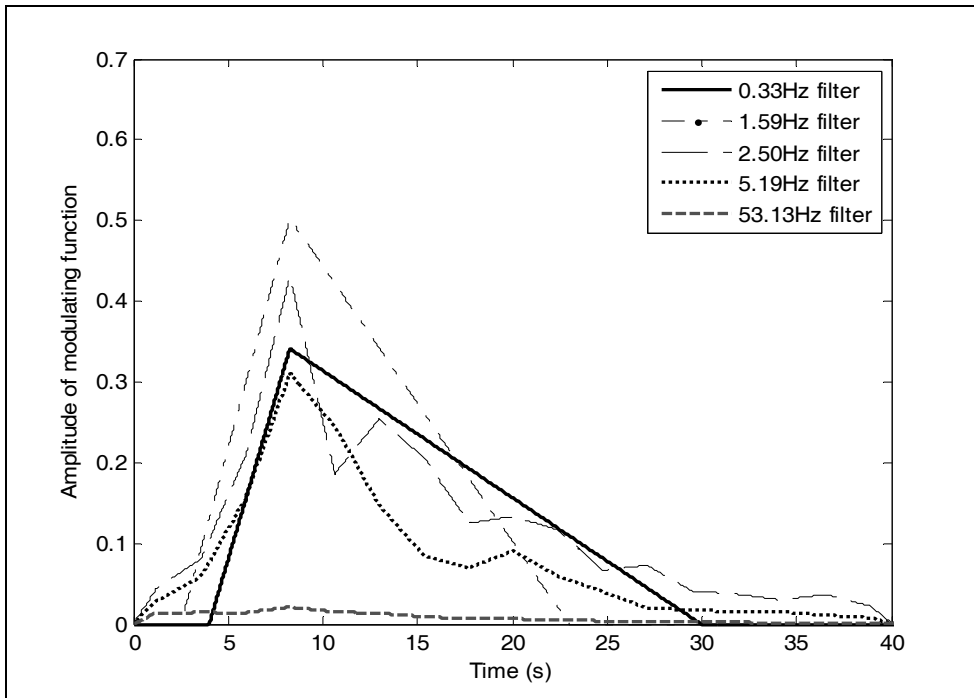
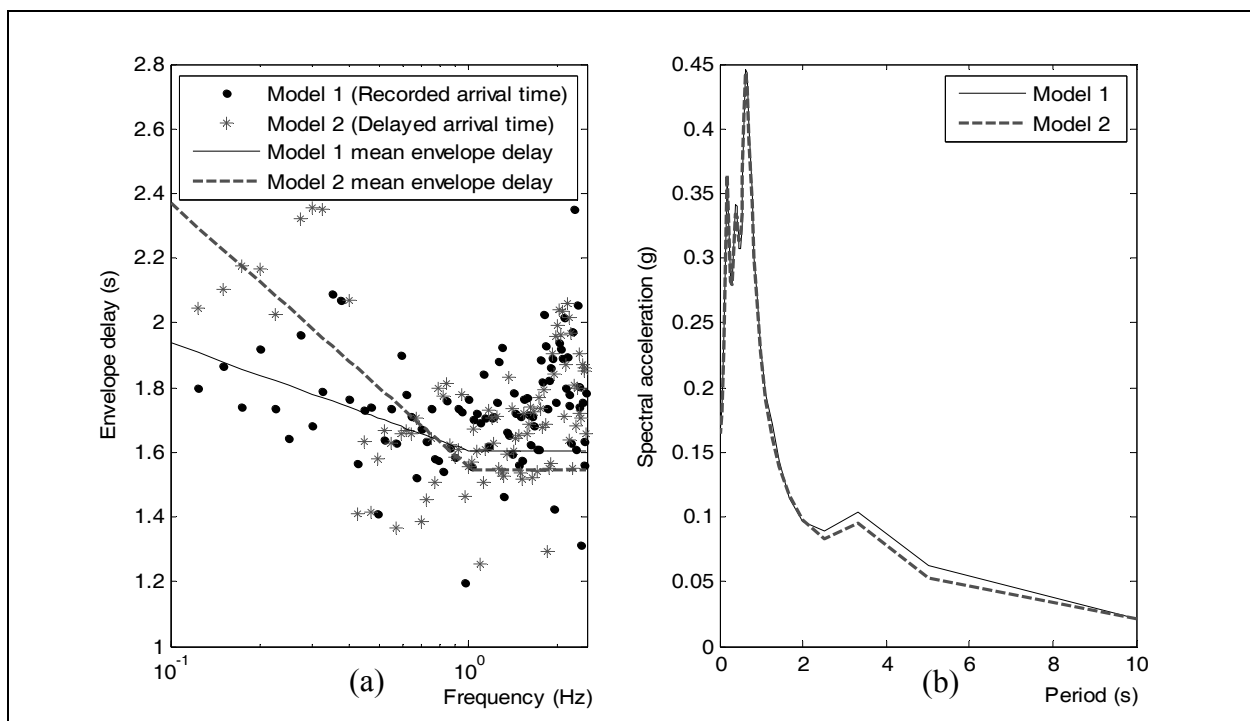Figure 2. Modulating functions for the ground motion simulations

Figure 3. a) Envelope delay of simulations of Model 1 (recorded arrival time) and Model 2 (delayed arrival time); b) Mean response spectra for the simulations of Model 1 and Model 2.

Fig. 3a illustrates the average envelope delays of the 100 simulations of Models 1 and 2. The simulations of Model 2 have the average slope as -0.3552, while slope for the simulations of Model 1 is -0.1451. As expected, the simulations of Model 2 exhibit higher spectral nonstationarity compared to those of Model 1. Fig. 3b shows the average response spectra of the simulations of Models 1 and 2. The amplitude of the pseudo spectral acceleration is expressed in the units of *g*, acceleration due to gravity. The response spectra from both of the models are practically same, expect in the long period region. This is due to the delay in the arrival time of the low frequency (long period) content. As the arrival time is delayed, the location of peak amplitude for the modulating function with the 0.33Hz (3s period) filter no longer coincides with the peak amplitudes of the rest of the modulating functions. Thus, the maximum intensity of the low frequency content is slightly reduced.

Structural Damage Measures

In the present study, three cumulative damage models are considered. The cumulative damage indices are based on 1) hysteretic energy dissipated (Kratzig et al. 1985), 2) plastic rotations (Mehanny and Deierlein 2001), and 3) a combination of hysteretic energy and peak deformation (Park and Ang 1985). In addition, the peak inter-storey drift ratio (lateral displacement/height) is considered as a non-cumulative measure for comparison.

A single-degree-of-freedom (SDOF) system is modeled with reinforced concrete section. The mass of the system is varied to alter its natural period, while maintaining 5% damping. The section is square with 200mm dimension and 3000mm height. The compressive strength of concrete is taken as 28MPa, while the yield strength of steel is 500MPa with a post-yield stiffness ratio of 5%. The 640 mm^2 area of steel is evenly distributed. The system is initially modeled as a the fiber-discretized section with individual fibers for concrete and reinforcing steel, This system is analyzed with the simulated ground motions based on Models 1 and 2.

Fig. 4 shows the "damage spectra" for the cumulative damage indices and the peak inter-storey drift ratio. As the delayed frequency content is 0.33Hz (3.0s period), the differences between Model 1 (solid line) and Model 2 (dotted line) are pronounced after the 3.0s period. It is evident in Figs. 4b, 4c and 4d that the longer periods undergo greater cumulative damage due to the spectral nonstationarity. In contrast, in Fig. 4a, the peak inter-storey drift ratio predicts higher damage for Model 1 when the period is longer than 4.5s. This indicates that the peak drift ratio may not reliably detect the influence of spectral nonstationarity on the structural damage.

In order to study the effect of hysteretic material model, the cross-section is also modeled with a tri-linear 'Hysteretic' material model in OpenSees (Mazzoni et al. 2009). The input values for the tri-linear hysteretic model are obtained from the section analysis. The system is analyzed with the same simulated ground motions as above. Figs. 5a and 5b show the damage spectra of the tri-linear hysteretic model with no stiffness degradation, and with the unloading stiffness degradation based on the ductility, respectively. The Mehanny-Deierlein (M-D) damage index is employed (Mehanny and Deierlein 2001). A comparison of Figs. 4c, 5a, and 5b clearly indicates that the section model with unloading stiffness degradation is most sensitive to the spectral nonstationarity. Thus, elastic-perfectly plastic models, with no stiffness degradation, may not consistently reveal the damage increment due to the spectral nonstationarity.
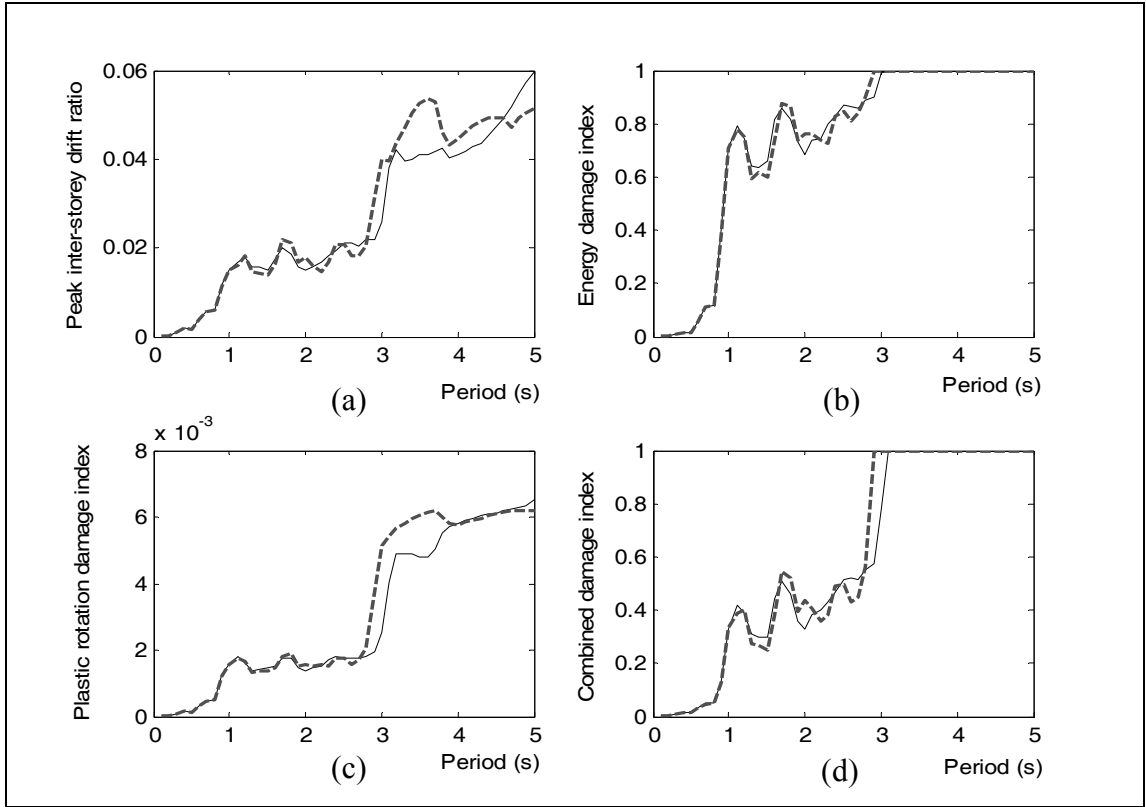
Figure 4. Variation of damage with the natural period of SDOF, a) Peak inter-storey ratio, b) Energy based damage index, c) Plastic rotations based damage index, d) Combined deformation and energy damage index. Solid line represents simulation from Model 1 (recorded arrival time) and dotted line represents the simulation from Model 2 (delayed arrival time).
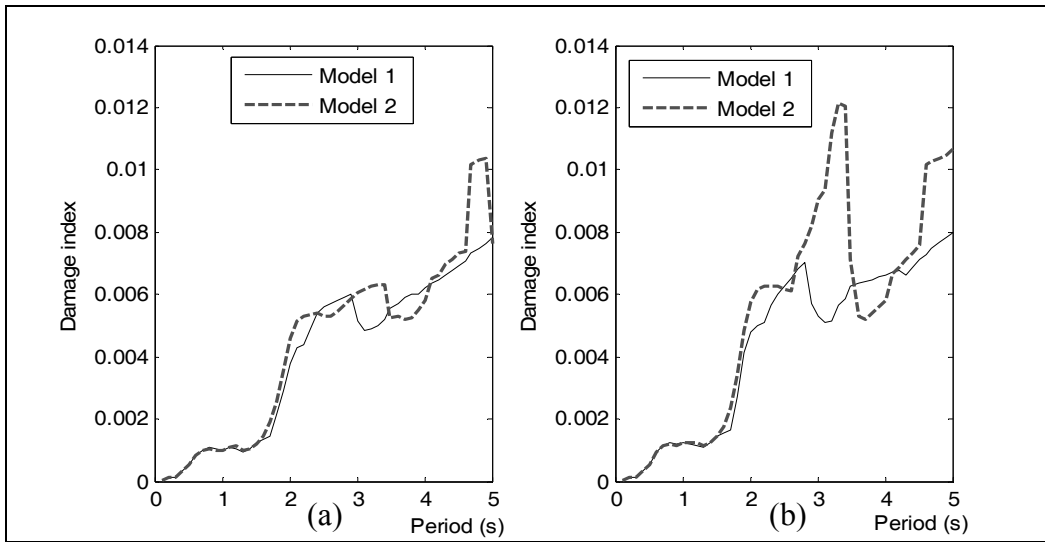

Figure 5. Damage spectra for hysteretic model with a) no stiffness degradation, b) unloading stiffness degradation

Numerical Example

A six storey reinforced concrete building in Vancouver, Canada is considered to illustrate the effects of spectral nonstationarity. The finite element model of the three-bay six-storey structure is shown in Fig. 6a. The section properties, design details and gravity loads are available in CPCA concrete design handbook (CPCA 1998). All the elements are modeled as nonlinear beam-column elements with fiber-discertized cross-sections in OpenSees (Mazzoni et al. 2009). The cross-sections are modeled with separate uniaxial material models for confined concrete, unconfined concrete, and reinforcing steel. A nonlinear dynamic analysis is performed with the simulated ground motions shown in Fig. 6b. As the same white noise variables, y_i, are employed in both the models, the simulated ground motions differ only in the arrival time of the low frequency content.
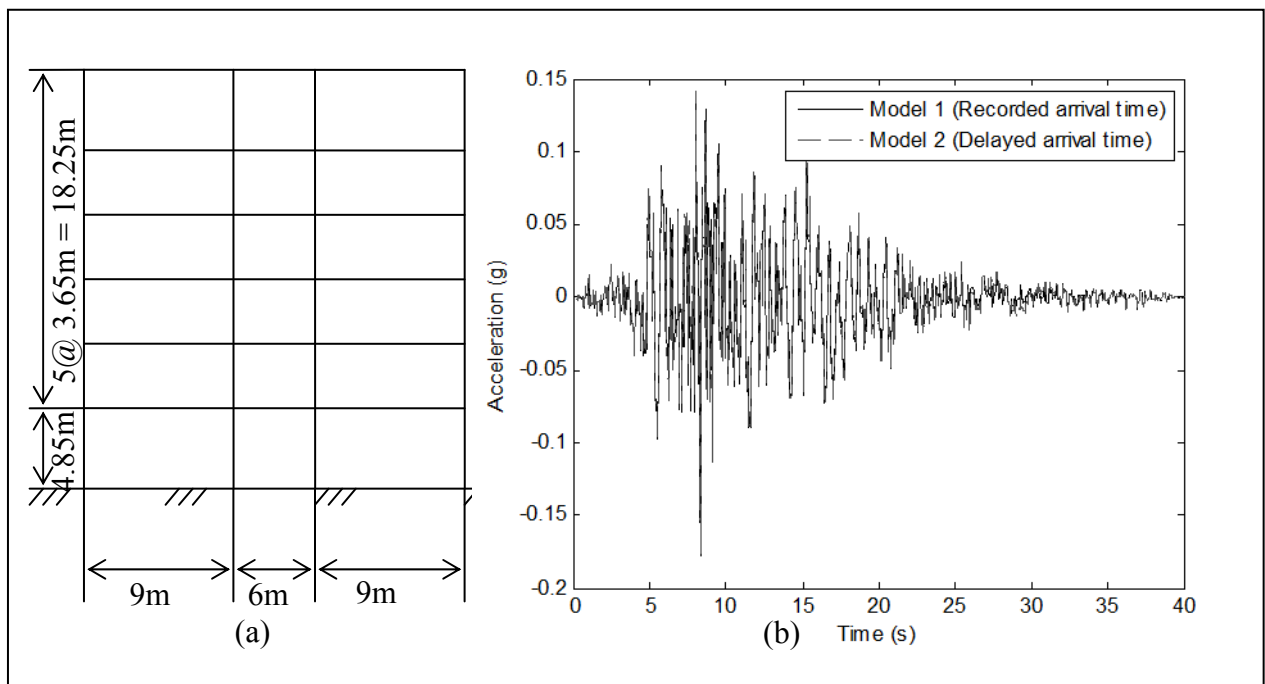

Figure 6. a) Finite element model of the six storey structure; b) Simulated ground motions with Model 1 (recorded arrival time) and Model 2 (delayed arrival time)

The cumulative damage in each member is computed as the Mehanny-Deierlein (M-D) damage index (Mehanny and Deierlein 2001). Fig. 7 shows the increment in the damage for the four columns in the first storey. It is evident that the ground motion with delayed arrival time causes higher damage. Especially in Fig. 7a, the left exterior column accumulates higher damage during the first 30s of the loading for Model 1 (solid line). However, after 30s, the intensity is practically zero for Model 1 and hence, there is no noticeable increase in the damage. In contrast, the damage continues to increase after 30s for Model 2 (dotted line) due to the presence of low frequency content.
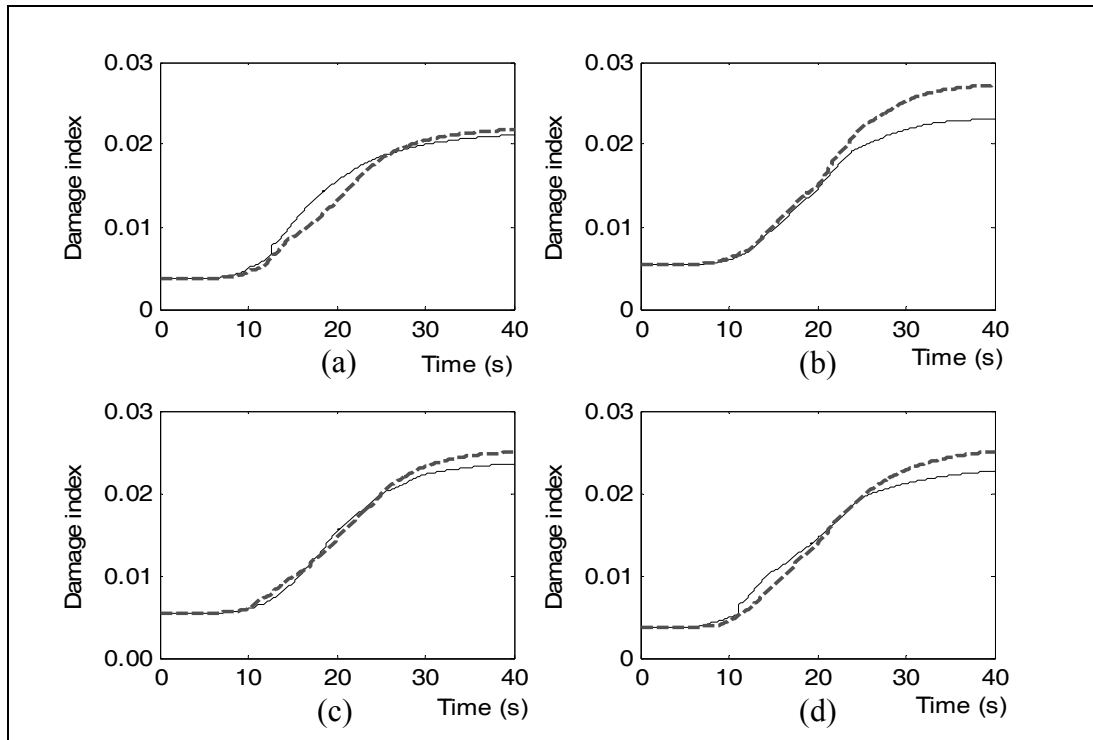
Figure 7. Evolution of M-D damage index with time in the first storey for, a) left exterior column, b) left interior column, c) right interior column, d) right exterior column; Solid line represents simulation from Model 1 (recorded arrival time) and dotted line represents the simulation from Model 2 (delayed arrival time).

Conclusions

This study indicates that the structural damage is sensitive to the arrival time of the low frequency content. Further research is required to understand the sensitivity of the structural damage to other measures of spectral nonstationarity, such as the location of peak amplitude, and the energy concentration. Additionally, the results indicate that the peak response measures and elastic-perfectly plastic section models may be inconsistent in detecting the vulnerability of a structure to the spectral nonstationarity.

References

Boore, D.M., 2003. Phase derivatives and simulation of strong ground motions, *Bulletin of the Seismological Society of America* 93 (3), 1132-1143.

Cao, H., and M. I. Friswell, 2009. The effect of energy concentration of earthquake ground motions on the nonlinear response of RC structures, *Soil Dynamics and Earthquake Engineering* 29, 292-299.

Conte, J.P., 1992. Effects of earthquake frequency non-stationarity on inelastic structural response, *Proceedings of the 10th World Conference on Earthquake Engineering*, A.A. Balkema, Rotterdam, The Netherlands.

CPCA (Canadian Portland Cement Association) 1998. Concrete Design Handbook. Canadian Portland Cement Association, Ottawa, Canada.

Iyama, J. and H. Kuwamura, 1999. Application of wavelets to analysis and simulation of earthquake motions, *Earthquake Engineering and Structural Dynamics* 28, 255-272.

Koduru, S.D., 2008. Performance-based earthquake engineering with the first order reliability method, *PhD Thesis*, University of British Columbia, Vancouver, Canada.

Kratzig, W.B., I.F. Meyer, and K. Meskouris, 1989. Damage evolution in reinforced concrete members under cyclic loading, *In A.H-S. Ang, M.Shizonuka & G.I. Schuller (eds), Structural Safety and Reliability: Proceedings of 5th International Conference on Structural Safety and Reliability (ICOSSAR '89), San Francisco, 7-11 Aug 1989*. American Society of Civil Engineers, New York.

Li, C.C., and A. Der Kiureghian, 1995. Mean out crossing rate of nonlinear response to stochastic input, *Proceedings of 7th International Conference on Applications of Statistics and Probability in Civil Engineering, Paris, France, July 10-13, 1995*. A.A.Balkema, Rotterdam, The Netherlands.

Mazzoni, S., F. McKenna, M.H. Scott, and G.L. Fenves, 2009. Open system for earthquake engineering simulation- User command-language manual, *OpenSees version 2.0*, Pacific Earthquake Engineering Research Center, University of California, Berkeley.

Mehanny, S.S.F., and G.G. Deierlein, 2001. Seismic damage and collapse assessment of composite moment frames, *Journal of Structural Engineering* 127(9), 1045-1053.

Mukherjee, S. and V.K. Gupta, 2002. Wavelet-based characterization of design ground motions, *Earthquake Engineering and Structural Dynamics* 31, 1173-1190.

Park, Y.J. and A.-H.S. Ang, 1985. Mechanistic seismic damage model for reinforced concrete, *Journal of Structural Engineering ASCE* 111, 722-739.

Rezaeian, S. and A. Der Kiureghian, 2008. A stochastic ground motion model with separable temporal and spectral nonstationarities, *Earthquake Engineering and Structural Dynamics* 37, 1565-1584.

Shrikande, M. and V.K. Gupta, 2001. On the characterization of the phase spectrum for strong motion synthesis, *Journal of Earthquake Engineering* 5 (4), 465-482.

Thrainsson, H. and A.S. Kiremidjian, 2002. Simulation of digital earthquake accelerograms using the inverse discrete Fourier transform, *Earthquake Engineering and Structural Dynamics* 31, 2023-2048.

Todorovska, M.I., H. Meidani, and M.D. Trifunac, 2009. Wavelet approximation of earthquake strong ground motion-goodness of fit for a database in terms of predicting nonlinear structural response, *Soil Dynamics and Earthquake Engineering* 29, 742-751

Wang, J., L. Fan, S. Qian, and J. Zhou, 2002. Simulations of non-stationary frequency content and its importance to seismic assessment of structures, *Earthquake Engineering and Structural Dynamics* 31, 993-1005.